# Resonance conditions for ^{93m}Mo isomer depletion via nuclear excitation by electron capture in a beam-based scenario

M. Polasik, K. Słabkowska, J. J. Carroll, C. J. Chiara, Ł. Syrocki, E. Węder, and J. Rzadkiewicz

Phys. Rev. C **95**, 034312 — Published 15 March 2017

DOI: 10.1103/PhysRevC.95.034312

# Resonance Conditions for $^{93m}$Mo Isomer Depletion via Nuclear Excitation by Electron Capture in a Beam-based Scenario

M. Polasik[1], K. Słabkowska[1], J.J. Carroll[2], C.J. Chiara[3], Ł. Syrocki[1], E. Węder[1], and J. Rzadkiewicz[4]
[1] *Faculty of Chemistry, Nicolaus Copernicus University in Toruń, 87-100 Toruń, Poland*
[2] *U. S. Army Research Laboratory, Adelphi, Maryland 20783, USA*
[3] *Oak Ridge Associated Universities, U. S. Army Research Laboratory, Adelphi, Maryland 20783, USA*
[4] *National Centre for Nuclear Research, 05-400 Otwock, Poland*
(Dated: February 28, 2017)

We present here a comprehensive analysis to understand the optimal atomic conditions for the first experimental observation of nuclear excitation by electron capture (NEEC) for the 6.85 h $^{93m}$Mo isomer with spin-parity $21/2^+$. NEEC process would provide an excitation from the long-lived isomer to a "depletion" level with spin-parity $17/2^+$ which lies only 4.85 keV higher in energy, and is itself a shorter-lived isomer that subsequently decays releasing a substantial amount of stored energy (2429.8 keV). The depletion level decays to a $13/2^+$ state through a 267.9 keV transition that offers the opportunity for identification of NEEC because it does not occur in the natural decay of the long-lived isomer. It has been shown that, for the proposed approach, high-precision atomic predictions are essential to understanding the proper physical conditions under which the experimental observation of the NEEC process will be possible using a beam-based scenario.

## I. INTRODUCTION

The ability to manipulate nuclear excitation and de-excitation, in particular the controlled release of energies up to a few MeV per nucleus, could open a wide range of applications such as nuclear batteries and $\gamma$-ray lasers [1-3]. One of the possible mechanisms for such an energy release is isomer depletion via nuclear excitation by electron capture (NEEC) [4-7], which is the inverse of the well-known internal conversion (IC) process. In the NEEC process, a free electron is captured into an unfilled atomic subshell of an ion with the simultaneous excitation of the nucleus. The NEEC process was predicted many years ago [4] and has been the subject of detailed theoretical studies (see e.g. [5-7]). However, NEEC has yet to be demonstrated experimentally. Attempts to observe NEEC in $^{242}$Am with an electron beam ion trap [8] or by fully stripped $^{57}$Fe ions channeling in a Si crystal [9] have been unsuccessful. It has been suggested that storage rings [10] or x-ray free-electron lasers [11] might be useful in the observation of NEEC.

Recently, in order to achieve a first experimental observation of the NEEC process, a new challenging approach was proposed [12]. A long-lived $^{93m}$Mo isomer (see Fig. 1) with a half-life of $T_{1/2} = 6.85$ h [12] would be produced on the fly via a reaction performed in inverse kinematics (heavy projectile nuclei incident on light target nuclei) so that isomeric nuclei would receive a high recoil energy. Passage of those recoiling ions through a medium would cause them to become highly ionized. Also, atomic electrons within the medium would approach the recoiling ions at a high velocity, as seen in the reference frame of the ions. Ultimately, the resonance condition for NEEC could be reached during the slowing of the recoiling ions within the medium. The long-lived $^{93m}$Mo isomer with spin-parity $21/2^+$ lies 2425.0 keV above the ground state and decays slowly via an $E4$ transition to a state with spin-parity of $13/2^+$. Its "depletion" level with spin-parity $17/2^+$ lies only 4.85 keV above the $^{93m}$Mo isomer, and is itself a shorter-lived isomer ($T_{1/2} \approx 3.5$ ns) that subsequently decays releasing a substantial amount of stored nuclear energy (2429.8 keV). The $17/2^+$ depletion level decays to a $13/2^+$ state through a 267.9 keV transition that offers a unique opportunity for identification of NEEC because it does not occur in the natural decay

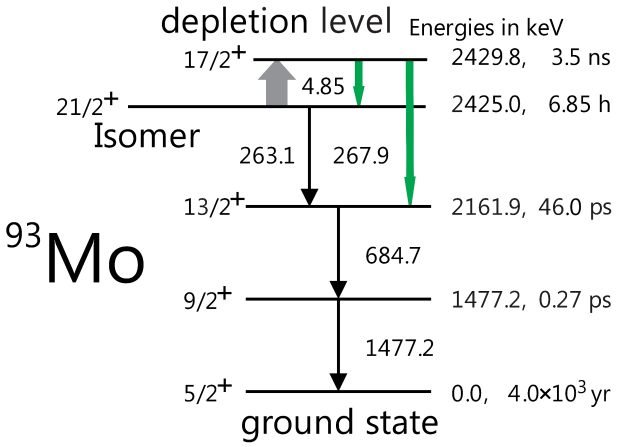


FIG. 1. (Color online) Partial level scheme (not to scale) for the $^{93}$Mo nucleus (Z=42). The grey arrow is the transition excited by NEEC, after production of the long-lived $^{93m}$Mo isomer, while the solid black arrows show the natural decay cascade from that isomer. The green transitions are unique signatures of NEEC that result in decay from the depletion level, once it is excited from the 6.85-h isomer. The right side of the figure gives the level energies (in keV) and half-lives, and the left side gives the angular momenta and parities, taken from [13].

of the long-lived isomer[1]. The energy of this transition is much larger than those of photons produced in radiative recombination, which are necessarily close in energy to the 4.85-keV $\gamma$ rays that could arise from the $17/2^+ \rightarrow 21/2^+$ decay transition from the depletion level. The $\gamma$ rays from that transition can only be emitted with very weak intensity as the decay rate is dominated by many orders of magnitude by IC and by the highly favored 267.9-keV $E2$ decay path (based on the $E_\gamma^5$ dependence for the $E2$ transition rates).

## II. $^{93m}$Mo ISOMER PRODUCTION

Figure 2 presents the experimental scheme for occurrence of the NEEC process proposed in Ref. [12]. A beam of some suitable higher-Z nucleus reacts with a lower-Z target to produce the $^{93m}$Mo isomer ions, which have very similar kinetic energies to that of the incident beam ions. The $^{93m}$Mo ions will then slow down in the stopping medium (solid or gas), which could be the same material as that serving for the isomer-producing nuclear reaction. The recently published Ref. [14] reiterates the approach discussed in Ref. [10], as well as another approach that is a modification of the beam-based scenario of Ref. [12], both within the context of storage rings.

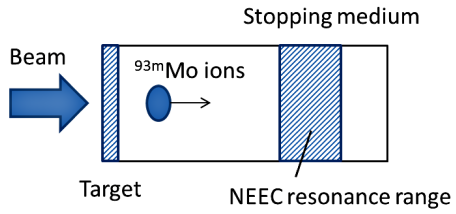


FIG. 2. General layout for experimental detection of the NEEC process as proposed in Ref. [12].

As an example, Fig. 3 presents the production cross sections predicted using the PACE4 code [15] for reactions resulting from $^{91}$Zr projectiles and $^4$He targets [12]. The production of the isotope $^{93}$Mo dominates over other nuclides for a wide range of beam energies, with the desirable $^{93m}$Mo isomer being most favored in the energy window from 600 to 700 MeV (6.6 to 7.7 MeV/nucleon). The $^{93m}$Mo ions have high recoil energies as this heavy reaction product takes most of the kinetic energy from the energetic $^{91}$Zr projectiles. For $^{91}$Zr beam ions at about 700 MeV, the mean recoil energy of $^{93}$Mo ions produced in He is about 660 MeV (7.1 MeV/nucleon).

[1] Other mechanisms, e. g. Coulomb excitation, could also excite the depletion level and their potential contribution to emission at 267.9 keV should be evaluated in the planning and analysis of any beam-based experiment.

## III. NEEC RESONANCE WINDOW WIDTHS

According to the approach depicted in Fig. 2, to achieve the resonance an electron with a specific kinetic energy ($E_{nl}^{kin}$) in the reference frame of the $^{93m}$Mo ion must be captured into a particular unfilled subshell with quantum numbers $n$ and $l$. The energy involved in this process, being the sum of the $E_{nl}^{kin}$ and energy released by electron capture into a given subshell ($E_{nl}^{released}$), must correspond, within the NEEC resonance window width ($\Gamma_{nl}^{NEEC}$), to the value (i.e., $\sim$ 4.85 keV) needed to excite the $^{93}$Mo nucleus, from the long-lived isomeric state ($21/2^+$) to the depletion state ($17/2^+$). A particular concern is that the $E_{nl}^{released}$ is highly discrete, with values that depend on the ionization degree ($q$) and on the specific electronic configuration of the Mo ion.

In general, as has been shown in Fig. 4, two radically different situations can be created: (i) an atomic excited state resulting from electron capture into a vacancy in a subshell other than the lowest one with an available vacancy, with the simultaneous excitation of the nucleus [Fig. 4(a)] or (ii) the atomic ground state resulting from electron capture into the lowest available vacant subshell, also with the simultaneous excitation of the nucleus [Fig. 4(b)]. In both cases, the nucleus can decay by the signature 267.9-keV transition after electron capture, while in case (i) the atomic system can also decay by x-ray emission. In either case the width of the NEEC resonance window is given by the sum of the atomic state width and the nuclear excited state width: $\Gamma_{nl}^{NEEC} = \Gamma_{nl}^{Atomic} + \Gamma_{Nuclear}$. However, the magnitude of $\Gamma_{nl}^{NEEC}$ is strongly affected by which case occurs. Table I

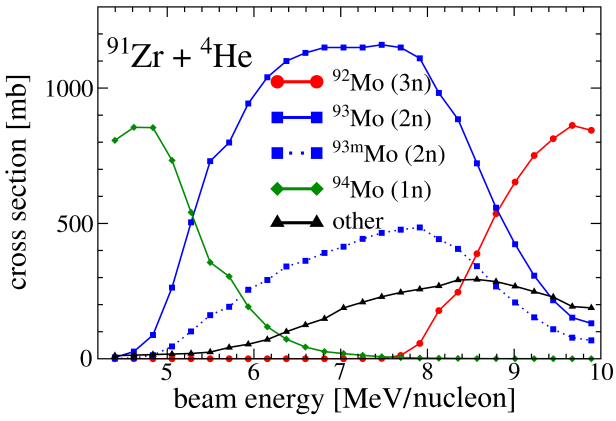


FIG. 3. (Color online) Cross section for the $^{91}$Zr + $^4$He beam-target reaction, calculated with the PACE4 code [15]. The total cross section leading to $^{93}$Mo (estimated to $^{93m}$Mo) is plotted with squares and a solid (dashed) blue line. The (3n), etc. in the legend refer to the evaporated nucleons from the nucleus due to the fusion-evaporation reaction modeled. The strongest competing reaction products are also indicated, with "other background" summing contributions from $^{93,94}$Nb and $^{90}$Zr.

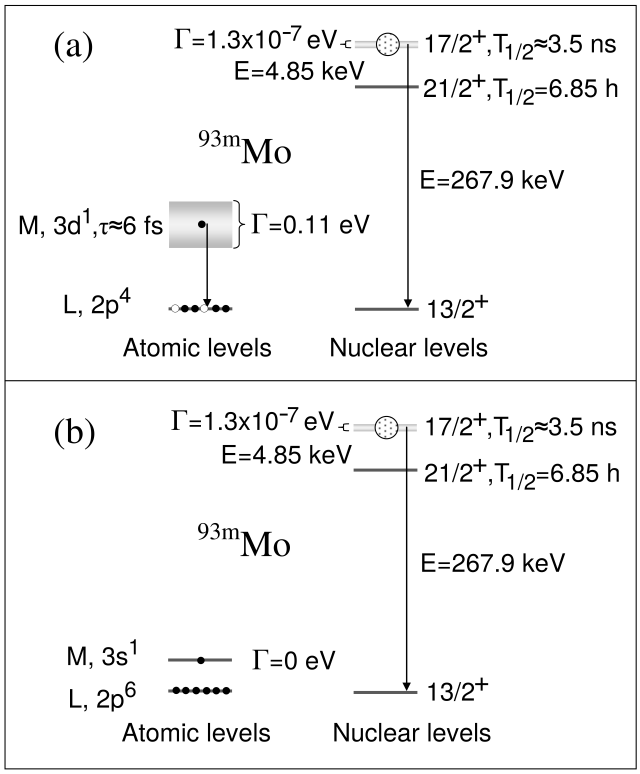


FIG. 4. Two scenarios for NEEC resonance window width. Panel (a) describes production, after free electron capture, of a double (atomic and nuclear) excited intermediate state for the $1s^22s^22p^43d^1$ excited atomic configuration of $^{93}$Mo ions ($\Gamma_{nl}^{Atomic} > 0$). Panel (b) describes production, after free electron capture, of an intermediate state which corresponds only to nuclear excitation. In this case, an electron has been captured into the 3s subshell of the $^{93}$Mo ion atomic ground state with $q = 32+$ for the $1s^22s^22p^6$ closed-shell configuration and, therefore, $\Gamma_{nl}^{Atomic} = 0$ (see Table I).

presents the atomic level widths, evaluated using the relativistic multiconfiguration Dirac-Fock (MCDF) method with the inclusion of Breit interaction and QED corrections [16-19], for electron capture into various $M$ and $N$ subshells ($\Gamma_{nl}^{Atomic}$) of Mo ions.

Figure 4(a) describes the production of a double (atomic and nuclear) excited intermediate state for the $^{93}$Mo ion. Starting in the $1s^22s^22p^4$ configuration with $q = 34+$, electron capture into the $3d$ subshell leads to the $1s^22s^22p^43d^1$ configuration and $q = 33+$, with the simultaneous excitation of the nucleus. As described above, when the atomic excited state can decay via x-ray emission, which is most often several orders of magnitude faster than low-energy nuclear transitions, the width of the NEEC resonance window can be approximated as $\Gamma_{nl}^{NEEC} \approx \Gamma_{nl}^{Atomic} = \Gamma_{3d}^{Atomic} = 0.11$ eV. This provides an enhancement to occurrence of the NEEC process. Such enhancement was previously noted [10] in the analysis of the potential observation for NEEC with U and Th nuclides. Moreover, in Ref. [10] the acronym NEECX was introduced to emphasize the role of a particularly fast subsequent atomic decay, which would under some circumstances prevent an IC channel for the slower nuclear decay from a depletion level. Generally, this IC blocking could enhance the overall $\gamma$ emission from a depletion level (although leaving the intrinsic $\gamma$ decay rate constant). However, for $^{93}$Mo the conversion coefficient for the 267.9 keV transition is relatively small ($\sim 0.0355$) and, furthermore, its value is not significantly changed by IC blocking by decay of the $3d$ subshell.

Figure 4(b) describes the capture of an electron into the lowest pre-capture subshell ($3s$), for a $^{93}$Mo ion in the $1s^22s^22p^6$ closed-shell configuration ($q = 32+$). In this case, the atomic ground state with the $1s^22s^22p^63s^1$ configuration is created and $\Gamma_{3s}^{Atomic} = 0$ (see Table I), and therefore, $\Gamma_{nl}^{NEEC} = \Gamma_{Nuclear} = 1.3\text{x}10^{-7}$ eV, due to the half-life of 3.5 ns for the nuclear depletion level in Fig. 4(b).

TABLE I. Predicted $\Gamma_{nl}^{Atomic}$ (in eV) for various $M$ and $N$ subshells of Mo ions from $q = 32+$ (i.e. $1s^22s^22p^6$ configuration) to $q = 36+$ (i.e. $1s^22s^22p^2$ configuration).

| Capturing | $q$ | | | | |
|---|---|---|---|---|---|
| $nl$ subshell | 32+ | 33+ | 34+ | 35+ | 36+ |
| $3s$ | 0.0000 | 0.0045 | 0.0067 | 0.0094 | 0.0116 |
| $3p$ | 0.00002 | 0.00003 | 0.00003 | 0.00003 | 0.00004 |
| $3d$ | 0.00003 | 0.11 | 0.11 | 0.11 | 0.11 |
| $4s$ | 0.0025 | 0.0033 | 0.0043 | 0.0054 | 0.0067 |
| $4p$ | 0.0026 | 0.0026 | 0.0027 | 0.0029 | 0.0033 |
| $4d$ | 0.0048 | 0.042 | 0.042 | 0.042 | 0.042 |

## IV. ION KINETIC ENERGY DECREASE NEAR THE NEEC RESONANCE

It is worth noting that the decrease of the $^{93m}$Mo ion kinetic energy as a result of collisions with the stopping medium occurs in discrete steps, further complicating the fulfillment of the NEEC resonance conditions during the stopping process. It is estimated that for a Mo ion at about 500 MeV (i.e., 5.4 MeV/nucleon) kinetic energy, the loss of energy in subsequent collisions occurs in small energy steps on the order of $\sim$ 1 keV per ion, which corresponds to changes on the order of $\Delta E^{kin} \sim 0.005$ eV in the apparent kinetic energies of the incident electrons, as seen in the reference frame of the $^{93m}$Mo ion.

Figure 5 illustrates the resonance conditions for $^{93m}$Mo ion energy release via the NEEC process with the size of the steps by which the ion kinetic energy decreases in the medium and for two different atomic NEEC resonance widths ($\Gamma_{3d}^{Atomic} \gg \Gamma_{3p}^{Atomic}$). The $E_{3d}^{kin}$ ($E_{3p}^{kin}$) means the contribution of electron kinetic energy to the total energy necessary to excite the nucleus as a result of electron capture into the $3d$ ($3p$) subshell for a particular $q$ of the $^{93m}$Mo isomer. The $E_{3d}^{kin}$ value must be higher than $E_{3p}^{kin}$ because the $E_{3d}^{released}$ is significantly lower than $E_{3p}^{released}$ (even for higher $q$ values). As can be seen from

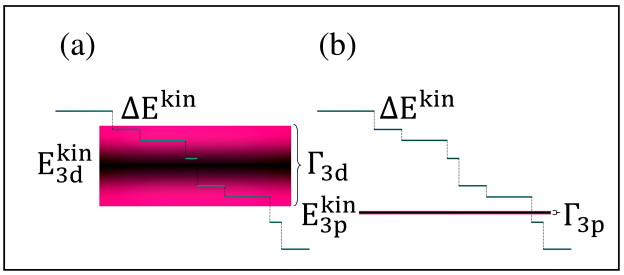


FIG. 5. (Color online) The resonance conditions for $^{93m}$Mo ion energy release via the NEEC process with a schematic depiction of the discrete but varying steps ($\Delta E^{kin}$) for ions slowing down in a medium near the NEEC resonance. Two cases are shown: (a) $\Gamma_{3d}^{Atomic} \gg \Delta E^{kin}$ and (b) $\Gamma_{3p}^{Atomic} \ll \Delta E^{kin}$ (see Table I). The $\Delta E^{kin}$ do not represent actual calculated steps.

Fig. 5(a), only a sufficiently wide NEEC width ($\Gamma_{nl}^{NEEC} \approx \Gamma_{nl}^{Atomic} = \Gamma_{3d}^{Atomic} \gg \Delta E^{kin}$) can ensure that the resonance conditions are achieved. Stated another way, if the $\Gamma_{nl}^{NEEC}$ is considerably smaller than $\Delta E^{kin} \sim 0.005$ eV [$\Gamma_{3p}^{Atomic} \ll \Delta E^{kin}$, as shown in Fig. 5(b)], the slowing ion could completely "hop" over the required energy, eliminating the possibility of NEEC. Therefore, the most promising for the NEEC process in $^{93m}$Mo ions is the $3d$ subshell, which has the largest $\Gamma_{nl}^{NEEC}$ (see Table I). Also promising seems to be capture into the $4d$ subshell. For the other subshells, the widths are a few orders-of-magnitude lower and are, hence, much less likely to find themselves at a NEEC resonance.

## V. NEEC RESONANCE CONDITIONS FOR DIFFERENT STOPPING MEDIA

A precise evaluation of the conditions necessary for the occurrence of the NEEC process in this beam-based scenario has to include consideration of the $^{93m}$Mo ion beam energy that can be achieved experimentally and the kind of stopping medium. A $^{93m}$Mo ion, after production in a nuclear reaction, travels through a material and loses energy. At the same time, the $q$ value of the $^{93m}$Mo ion significantly changes as a function of kinetic energy. For the energies relevant to the NEEC process for $^{93m}$Mo ions, Fig. 6 shows the mean equilibrium charge state ($q_{mean}$) of the $^{93m}$Mo recoil ion as a function of its kinetic energy in two stopping media, predicted using Schiwietz and Grande formulas [20] for gas (He) and solid (C) targets. The absolute uncertainties $\Delta q_{mean}$ are 0.48 for He gas and 0.54 for C solid targets [20], and this range is shown in Fig. 6 by the dashed lines near the solid ones. Moreover, we have estimated the widths of the $q$ distribution (FWHM) to be 1.81 for He gas target [21] and 1.50 for C solid target [22,23]. They are presented in Fig. 6 as the short dashed lines with the descriptions: "$q_{mean}$-FWHM/2" and "$q_{mean}$+FWHM/2".

Demanding that the cross section for the production of $^{93m}$Mo ions in a $^{4}$He gas target exceeds that of any other

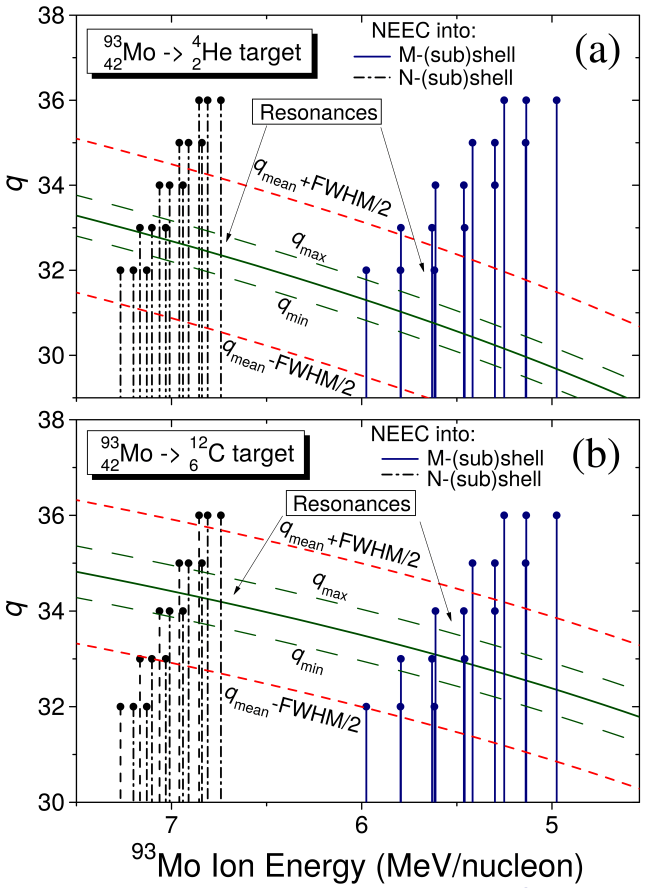


FIG. 6. (Color online) Predicted $q_{mean}$ of a $^{93m}$Mo ion as a function of its kinetic energy for He gas (top) and C solid (bottom) stopping media. The vertical bars present the potential positions of the $^{93m}$Mo ion NEEC resonance kinetic energies, which can occur for $q$ (vertical axis), from $q = 32+$ to $q = 36+$ as indicated when the tops of the bars are within the $q$ range. Each set of three bars represents, from left to right, electron capture into the $d$, $p$, and $s$ subshells.

nucleus produced in this reaction sets the incident $^{91}$Zr beam energy (see Fig. 3), and limits the maximum recoil energy of a $^{93m}$Mo ion to ~7.7 MeV/nucleon. Figure 6 clearly shows that the line representing the predicted $q_{mean}$ monotonically decreases during the stopping process in both media. As can be seen, higher $q_{mean}$ have been produced in the case of $^{93m}$Mo ions passing through a C solid target than a He gas target. For recoil energies around 7 MeV/nucleon, the $q_{mean}$ ~32.8 and $q_{mean}$ ~34.5 for He and C targets, respectively.

The discrete $E_{nl}^{released}$ energies as a function of $q$, for different $M$ and $N$ subshells of a $^{93m}$Mo ion, have been obtained using the relativistic MCDF method [16-19]. Then all potentially possible NEEC resonance energies, i.e. the specific electron kinetic energy, $E_{nl}^{kin}$, for $q = 32+$ up to $q = 36+$ of $^{93m}$Mo ions have been evaluated (using values of $E_{nl}^{released}$). From the left to right side of Fig. 6, the positions of the vertical bars indicate the poten-

tial $^{93m}$Mo ion kinetic energies (obtained on the basis of $E_{nl}^{kin}$) for which the NEEC resonance could occur for electrons captured to the $4d$, $4p$, and $4s$, and the $3d$, $3p$, and $3s$ subshells. The heights of the bars indicate the value of $q$ for which the capture could occur into the specific subshell.

One of the important criteria that precisely establishes in Fig. 6 the optimal conditions for the NEEC process in the case of electron capture to a given ($N$ or $M$) subshell is the location of the tops of the bars (for specific charge state of the $^{93m}$Mo ion) relative to the central line corresponding to the predicted $q_{mean}$ of the $^{93m}$Mo ion projectile as a function of its kinetic energy in the stopping medium. For a He gas target, the potential positions of the $^{93m}$Mo ion NEEC resonance kinetic energies can mostly be achieved in the case of electron capture into the $N$ subshells. This can be seen in Fig. 6(a) by the proximity of the bar tops of the $4d$, $4p$, and $4s$ subshells for $q = 33+$ to the line representing the $^{93m}$Mo ion $q_{mean}$, with the energy for the $4d$ subshell falling closest to the line. However, for the He gas target, electron capture into the $M$ shell is barely possible [see Fig. 6(a)]. It is worth underlining that the most probable case seems to be electron capture into the $4d$ subshell because of the large NEEC window width, i.e. $\Gamma_{nl}^{NEEC} \approx \Gamma_{4d}^{Atomic} = 0.042$ eV (see Table I).

For a solid C target, the potential positions of the $^{93m}$Mo ion NEEC resonance kinetic energies seem to be achievable in the case of electron capture into the $M$ subshells (i.e. $3d$, $3p$, or $3s$) for $q = 33+$ because of the proximity of the bar tops to the line representing the $^{93m}$Mo ion $q_{mean}$ [see Fig. 6(b)]. Moreover, we can suppose (see Fig. 6) that for the C solid target the electron capture to the $N$ shell seems to be less likely. We can also see for $q = 33+$ that the top of the bar for electron capture to the $3d$ subshell is located slightly farther from the line representing the $q_{mean}$ than for the $3p$ and $3s$ subshells. Therefore, for electron capture to the $3d$ subshell, fewer ions (than for electron capture to $3p$ or $3s$) may participate in the NEEC resonance process. It should be noted that, in order to estimate the NEEC process probability for electron capture to any $M$ or $N$ subshells, we also have to take into consideration the resonance window widths which are more fundamental than the energetic condition discussed above. Therefore, the most probable scenario for the C solid target seems to be electron capture to the $3d$ subshell, despite fewer ions participating in the process, because the resonance window is much larger for the $3d$ subshell ($\sim 0.11$ eV) than for the $3p$ ($\sim 0.00003$ eV) or the $3s$ (0.0045 - 0.0116 eV) subshells.

## VI. SUMMARY AND CONCLUSIONS

The detailed study presented above has shown the crucial role of complex atomic processes in ensuring that resonance conditions would be satisfied in an experimental demonstration of the NEEC process. In order to observe the NEEC process for the first time, an approach has been proposed here, adapting that introduced in Ref. [12] with detailed quantitative analysis of atomic conditions for gas and solid stopping media, for the long-lived $^{93m}$Mo isomer with spin-parity $21/2^+$. Its "depletion" level with spin-parity $17/2^+$ lies only 4.85 keV above the $^{93m}$Mo isomer, and is itself a shorter-lived isomer that subsequently decays releasing a substantial amount of stored nuclear energy (2429.8 keV). The $17/2^+ \rightarrow 13/2^+$ decay path offers a unique opportunity for identification of NEEC because it does not occur in the natural decay of the long-lived isomer.

As presented in Sec. III, an atomic excited state, created as a result of electron capture into a vacancy in a subshell higher in energy than the lowest possible one (with the simultaneous excitation of the nucleus), can decay via x-ray emission, which is most often several orders-of-magnitude faster than the low-lying nuclear states. However, also crucial for understanding the resonance conditions for $^{93m}$Mo ion energy release via the NEEC process is a detailed analysis of the decreasing steps in kinetic energy near the NEEC resonance energy. As has been explained in Sec. IV, the resonance conditions can be achieved only if a NEEC resonance window width is sufficiently wide. We have found, for the first time, that the most promising atomic subshells into which an electron can be captured for the NEEC process in $^{93}$Mo ions are the $3d_{3/2,5/2}$ states (because of the largest atomic level widths). Also promising seems to be capture into the $4d_{3/2,5/2}$ states.

A fundamental step in designing the optimal conditions for the first observation of the NEEC process in beam-based scenarios is to take into account a beam of some suitable higher-Z nucleus reacting with a lower-Z target to produce the $^{93m}$Mo isomer (with the initial recoil kinetic energy of ions which exceed the NEEC resonance energy). The most probable case seems to be the choice of C solid target and the electron capture into the $3d$ subshell because of the largest NEEC resonance window.

Finally, one can expect that the results of a successful search for evidence of the NEEC process would not only provide identification of a new physical phenomenon, but also would be a starting point for applied research into the controlled release of energy stored in certain nuclear isomers, which would provide an important step towards the development of a new, unconventional nuclear battery.

## ACKNOWLEDGMENTS

This work is supported by the Polish National Science Center under Grant No. 2011/01/D/ST2/01286 and by the U. S. Army Research Laboratory under Cooperative Agreements W911NF-12-2-0019 and W911NF-16-2-0008.

[1] J. J. Carroll, S. A. Karamian, L. A. Rivlin, and A. A. Zadernovsky, Hyperfine Interact. **135**, 3 (2001).

[2] A. Aprahamian and Y. Sun, Nature Phys. **1**, 81 (2005).

[3] P. M. Walker and G. D. Dracoulis, Nature **399**, 35 (1999).

[4] V. I. Goldanskii and V. A. Namiot, Phys. Lett. B **62**, 393 (1976).

[5] A. A. Zadernovsky and J. J. Carroll, Hyperfine Interact. **143**, 153 (2002).

[6] A. Pálffy, W. Scheid, and Z. Harman, Phys. Rev. A **73**, 012715 (2006).

[7] A. Pálffy, J. Evers, and C. H. Keitel, Phys. Rev. Lett. **99**, 172502 (2007).

[8] L. Bernstein, "EBIT Plans in Livermore and Berkeley."in Proc. of the ECT Workshop on Atomic Effects inNuclear Excitation and Decay, Trento, Italy, June 15-19, 2009, www.ect.it, under link to meetings for 2009.

[9] P. Morel, J. M. Daugas, G. Gosselin, V. Méot, and D. Gogny, AIP Conf. Proc. **769**, 1085 (2005).

[10] A. Pálffy, Z. Harman, C. Kozhuharov, C. Brandau, C. H. Keitel, W. Scheid, and T. Stöhlker, Phys. Lett. B **661**, 330 (2008).

[11] J. Gunst, Y. A. Litvinov, C. H. Keitel, and A. Pálffy, Phys. Rev. Lett. **112**, 082501 (2014).

[12] S. A. Karamian, J. J. Carroll, Physics of Atomic Nuclei **75**, 1362 (2012).

[13] C. M. Baglin, Nucl. Data Sheets **112**, 1163 (2011).

[14] M. Lestinsky, V. Andrianov, B. Aurand, V. Bagnoud, D. Bernhardt, H. Beyer, S. Bishop, K. Blaum, A. Bleile, At. Borovik Jr., F. Bosch, C. J. Bostock, C. Brandau, A. Bräuning-Demian, I. Bray, T. Davinson, B. Ebinger, A. Echler, P. Egelhof, A. Ehresmann, M. Engström, C. Enss, N. Ferreira, D. Fischer, A. Fleischmann, E. Förster, S. Fritzsche, R. Geithner, S. Geyer, J. Glorius, K. Göbel, O. Gorda, J. Goullon, P. Grabitz, R. Grisenti, A. Gumberidze, S. Hagmann, M. Heil, A. Heinz, F. Herfurth, R. Heß, P.-M. Hillenbrand, R. Hubele, P. Indelicato, A. Källberg, O. Kester, O. Kiselev, A. Knie, C. Kozhuharov, S. Kraft-Bermuth, T. Kühl, G. Lane, Yu. A. Litvinov, D. Liesen, X. W. Ma, R. Märtin, R. Moshammer, A. Müller, S. Namba, P. Neumeyer, T. Nilsson, W. Nörtershäuser, G. Paulus, N. Petridis, M. Reed, R. Reifarth, P. Reiß, J. Rothhardt, R. Sanchez, M. S. Sanjari, S. Schippers, H. T. Schmidt, D. Schneider, P. Scholz, R. Schuch, M. Schulz, V. Shabaev, A. Simonsson, J. Sjöholm, Ö. Skeppstedt, K. Sonnabend, U. Spillmann, K. Stiebing, M. Steck, T. Stöhlker, A. Surzhykov, S. Torilov, E. Träbert, M. Trassinelli, S. Trotsenko, X. L. Tu, I. Uschmann, P. M. Walker, G. Weber, D. F. A. Winters, P. J. Woods, H. Y. Zhao, Y. H. Zhang, for the CRYRING@ESR Research Community, Eur. Phys. J. Special Topics **225**, 797-882 (2016).

[15] O. B. Tarasov and D. Bazin, Nucl. Instrum. Meth. Phys. Res. B **204**, 174 (2003).

[16] I. P. Grant and H. M. Quiney, Adv. At. Mol. Phys. **23**, 37 (1988).

[17] K. G. Dyall, I. P. Grant, C. T. Johnson, F. A. Parpia, and E. P. Plummer, Comput. Phys. Commun. **55**, 425 (1989).

[18] M. Polasik, Phys. Rev. A **39**, 616 (1989); **39**, 5092 (1989); **40**, 4361 (1989); **41**, 3689 (1990); **52**, 227 (1995).

[19] M. Polasik, K. Słabkowska, J. Rzadkiewicz, K. Kozioł, J. Starosta, E. Wiatrowska-Kozioł, J.-Cl. Dousse, J. Hoszowska, Phys. Rev. Lett. **107**, 073001 (2011).

[20] G. Schiwietz and P. L. Grande, Nucl. Instrum. Meth. Phys. Res. B **175-177**, 125 (2001).

[21] H. Kuboki, H. Okuno, H. Hasebe, N. Fukunishi, E. Ikezawa, H. Imao, O. Kamigaito, and M. Kase, Phys. Rev. ST Accel. Beams **17**, 123501 (2014).

[22] J. Braziewicz, M. Polasik, K. Słabkowska, U. Majewska, D. Banaś, M. Jaskóła, A. Korman, K. Kozioł, W. Kretschmer, and J. Choinski, Phys. Rev. A **82**, 022709 (2010)

[23] K. Shima, N. Kuno, M. Yamanouchi, and H. Tawara, At. Data Nucl. Data Tables **51**, 173 (1992).